Volume 3 Issue 2 (September 2023)
DOI 10.24191/jaeds.v3i2.66
eISSN 2805-5756

Journal of Applied Engineering Design & Simulation

Analytical Prediction of Fatigue Resistance of Additively Manufactured Aluminium Alloy Based on Murakami Method

Matthias Oberreiter[1], Nik Nur Khaleeda[3*], Michael Stoschka[1], Yupiter HP Manurung[2,3], Mohd Shahriman Adenan[2,3], Renga Rao Krishnamoorthy[2,4]

[1]Chair of General Mechanical Engineering, Montanuniversität Leoben, 8700, Austria.
[2]Smart Manufacturing Research Institute, Universiti Teknologi MARA, Shah Alam 40450 Selangor, Malaysia.
[3]School of Mechanical Engineering, Universiti Teknologi MARA, Shah Alam 40450 Selangor, Malaysia.
[4]School of Civil Engineering, Universiti Teknologi MARA, Shah Alam 40450 Selangor, Malaysia.
*corresponding author: khaleedazainal@gmail.com

ABSTRACT

This research is devoted to analyze the stress state and fatigue strength of two specimens made by a newly developed high-strength aluminium alloy produced by the wire arc additive manufacturing (WAAM) process. The relationship between fatigue strength and flaw size was calculated based on the root squared area – a parameter by conventional Murakami's equation which is a widely used analytical approach for predicting fatigue resistance in metallic materials. The research involves the metallographic preparation process on two aluminum alloy labeled HS-Al-A and HS-Al-B followed by Vickers hardness measurement. Further, the image of the observed pores was processed and dimensioned using an open-sourced software ImageJ by considering pixels and actual distance as well as by defining image threshold value for measuring pore sizes. The analytical approach is conducted in order to describe the maximum stress intensity factor K_{max} at the crack front and to assess the fatigue strength σ_{FS}. As final results, specimen A has an average pore area of ≈65 µm with K_{max} of 333.75 MPa·√m and σ_{FS} of 137 MPa, while specimen B has an average pore area of ≈42 µm with K_{max} of 325.13 MPa·√m and σ_{FS} of 153 MPa. Overall, this research allows the formulation of a method for estimating fatigue strength of large defects leading to a conclusion that flaws can influence the fatigue resistance of the material so that the bigger the flaw size is, the lower σ_{FS} and the higher the K_{max}.

Keywords: Murakami; Fatigue Strength; Stress Intensity Factor; ImageJ

Nomenclature

σ_{FS}	Fatigue Strength (MPa)
$\sqrt{area_{max}}$	Square root maximum area of pore (µm)
HV	Hardness value (kgf/mm^2)
ΔK_{eff}	Effective stress intensity factor
K_{max}	Maximum stress intensity factor
$\Delta\sigma_c$	Crack closure

Abbreviations

WAAM	Wire arc additive manufacturing
OPS	Oxide polishing suspensions
LOM	Light optical microscopy
MSRAP	Maximum square root area of pores
LEVD	Largest extreme value distribution

Received on 29.08.2023
Accepted on 19.09.2023
Published on 22.09.2023

1.0 INTRODUCTION

Surface roughness or defects, which are inevitably produced by the manufacturing process, are the drawback or difficulty of additive manufacturing. Considering fatigue is a local phenomenon that begins with microstructural inhomogeneities or the existence of stress raisers (inclusions and pores) that can cause cracks to form or develop, the issue of fatigue resistance and the scatter of fatigue attributes are inextricably linked [1]. Almost all fatigue initiates on the surface of a material. In many typical loading situations such as bending and torsion, the surface experiences the highest stress, making it reasonable for the failure to initiate there [2]. The threshold (or non-propagation) condition of those short cracks is the fatigue strength. The fatigue strength of materials is commonly described as the highest stress amplitude that the material can endure without experiencing failure within a specific number of loading and unloading cycles, such as 10^7 or 10^9 [3]. The size of the crack, once it has started from a defect, influences the level of stress intensification at the crack tip and, consequently, the threshold condition, which has a significant impact on the fatigue strength [4].

Wire arc additive manufacturing (WAAM) is a relatively new technology for the production of metal components. Although it offers numerous advantages, such as high deposition rates and the ability to produce complex geometries, the mechanical properties of WAAM materials are not yet fully understood [5], [6].This lack of knowledge presents a challenge when it comes to the design and engineering of components made using WAAM. One of the key mechanical properties that needs to be understood is the fatigue strength of WAAM materials. The microstructure and defects of WAAM materials can differ significantly from those of conventionally produced materials, making it difficult to predict their fatigue behaviour accurately [7]. Many attempts have been made to determine the fatigue strength in a cost-effective way relating fatigue strength to other mechanical properties, such as yield strength, tensile strength, hardness and so on. Accordingly, the relations between fatigue strength and other mechanical properties have been of more interest.

For the prediction of fatigue strength, the size of the maximum defect must be predicted. The most practical size parameter for defects is the square root of the defect projection area, which projects defects onto the plane perpendicular to the direction of maximum stress [8]. Several studies have applied the Murakami method to analyse the fatigue behaviour of WAAM materials, including aluminium alloy [6], [9], [10]. An important finding by Murakami is that there is a quantitative relationship among fatigue strength, hardness HV and inclusion size $\sqrt{area_{max}}$ in high strength steels. For example, a study conducted by Rhein et al. [11] used the Murakami method to analyse the effect of process parameters on the fatigue behaviour of an AlSi10Mg WAAM alloy. The study found that the Murakami method provided a reliable tool for predicting the fatigue behaviour of the material, and that the fatigue strength was influenced by the microstructure and porosity of the material. However, if the size of those undesirable features had not been able to be determined, this successful approach would lack applicability. Therefore, by applying the Murakami approach on the high-strength aluminium alloy allows for evaluation of the fatigue strength of the material based on the defect size area.

2.0 EXPERIMENTAL SETUP AND PROCEDURE

The experiment setup and procedure for the application of Murakami method in evaluating the fatigue strength of the aluminium alloy labelled HS-Al-A and HS-Al-B is divided into three phases. The first phase is the sample preparation by metallography process which helps in the study of the material microstructure. The material microstructure is the most important feature for the design of engineering structures with advanced performances. The process involves five steps to be included in the preparation. The second phase involves analysis of the microstructure using ImageJ which is an open software for image processing that aids in determining and evaluating the microstructure and defect size of WAAM aluminium alloy. The next phase will proceed when the analysis is successful with no error encountered from the result obtained. Lastly, the result of the image processing is used for the application of the Murakami method. The relationship between the fatigue strength and the properties of the microstructure is an important concern in fatigue analysis.

2.1 Metallography analysis process

Microstructural analysis will be used to determine the cause of the failure; thus, samples should be taken from the region that will yield the most details. The first step in the preparation of a metallographic samples is sectioning and cutting. Referring to Figure 1, the part or solid body is typically too large for the subsequent metallographic grinding and polishing stages to be performed; thus, this step is necessary. The best way to eliminate these undesirable features is through abrasive cutting (sectioning) which produces a smooth surface and operates rapidly.

By cutting, the statics of extreme values of defects can be obtained. In situations when the heat produced by conventional abrasive cutters must be avoided, low-speed cut off wheel are used. In all sectioning operations, sufficient coolant and appropriate speed control are required. Figure 2 below shows the machine used and direction of the specimen for cutting process.

The technical field of microscopy involves using microscopes to show significant difference and regions of specimen that are not visible to the naked eye. When electromagnetic radiation interacts with a specimen through a single lens or multiple lens allow a magnified view of sample, optical microscopy entail the capturing of the scattered radiation or another signal in order to form an image. To understand the microstructure or nanostructure of materials, chemicals, or products requires microscopy analysis. Data and image captured by digital microscope from the microscopy analysis is important for the research of fatigue strength as it does not only focus on the microstructure but also the inhomogeneities, inclusion, defects, etc. Advanced microscopy instruments, specialised cameras, and image analysis software are needed for efficient digital microscopy analysis. The microstructure image of the aluminium specimen was done using Keyence digital microscope. At the touch of a button, a 4K High Accuracy digital microscope may record images with high resolution and measurement data for inspection and failure analysis. Figure 3 show the starting of the fatigue crack until the final breakage. These cracks propagate beyond grain boundaries until they lead the specimen to fracture.

Figure 1. Fatigue test specimen of high-strength aluminium alloy

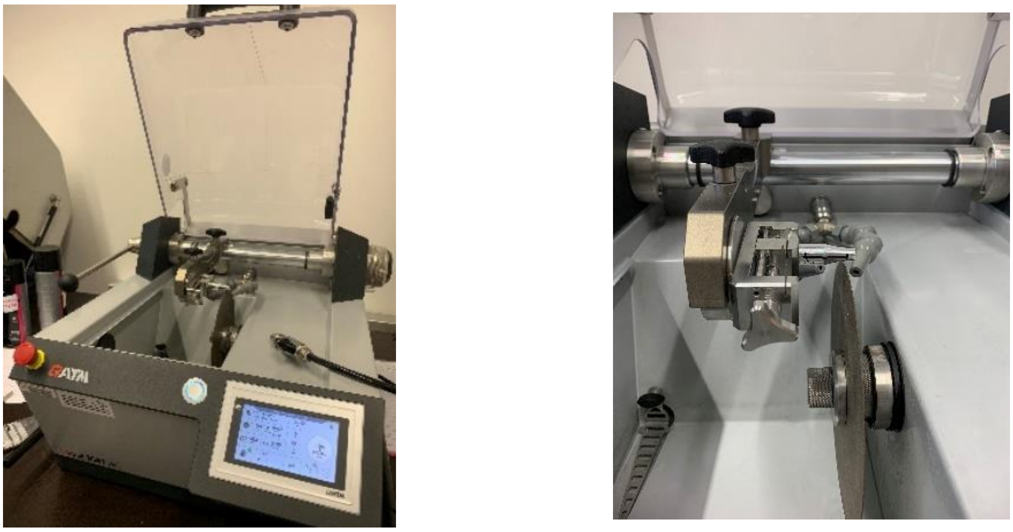

(a) (b)

Figure 2. Sectioning and cutting process - (a) Precision cutting machine; (b) Section to be cut

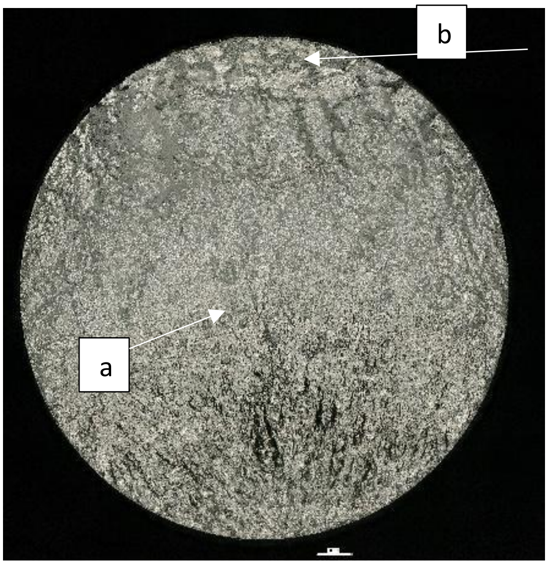

Figure 3. Fractured surface of aluminium – a) starting of fatigue crack; b) final breakage

The starting of a fatigue crack is darker than the final breakage is due to the process of crack propagation. In the early stages of fatigue, a small crack begins to form on the surface of the material due to cyclic loading. This crack is typically small and shallow, and it creates a stress concentration in the material that leads to further crack growth. As the crack propagates through the material, the stresses at the crack tip increase, and the crack begins to grow more rapidly. This rapid growth causes the crack tip to become sharper and more pointed, which results in a change in the surface appearance of the material. The final breakage occurs when the stress concentration at the crack tip becomes so severe that the material can no longer withstand the applied loads, and the material fails catastrophically. At this point, the crack tip has become extremely sharp, and the surface of the material may appear brighter or more reflective due to the deformation and fracture of the material.

Small samples are typically mounted in plastic for ease of handling and to safeguard the prepared specimen's edges. Specimens are frequently enclosed in rigid polymer with a diameter of 1 to 1.5 inches using compression moulding. The materials used in compression moulding can either be thermosetting or thermoplastic. The difference during mounting is time because the pressure and moulding temperature are kept constant. The aluminium alloy specimen is put inside the mounting cylinder and later filled with a pre-measured amount of powder resins. To complete the polymerization process and solidly encase the aluminium alloy specimen, the mounting cylinder is then sealed, compressed and heated. The time taken for the mounting was 10 minutes in which the first 5 minutes is for the heating process and the remaining 5 minutes for cooling at a temperature of 180°C. Figure 4 shows the process of mounting the HS-Al specimen using the hot mounting press machine.

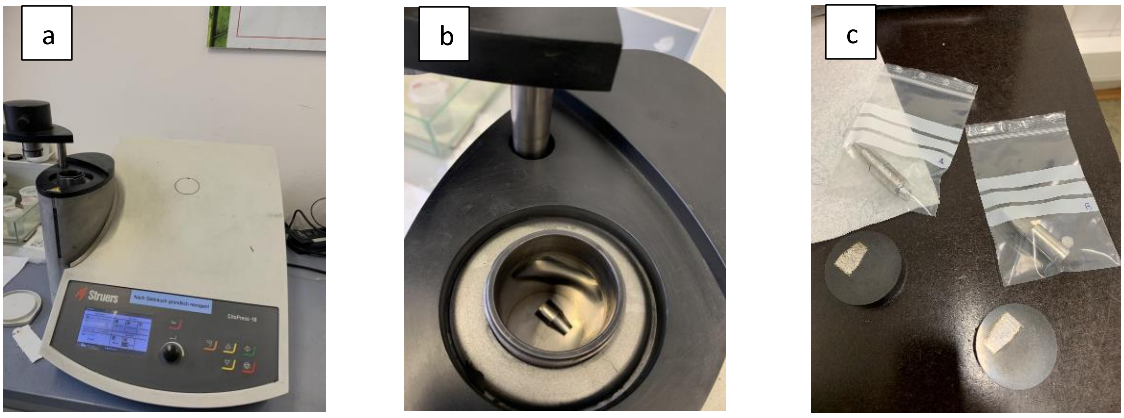

Figure 4. Mounting process – a) Hot mounting press machine; b) Surface to be analyse facing down; c) Mounted HS-Al specimen

The aluminium alloy specimens are grinded to remove the rough surface to create a smooth surface. The entire metallographic sample preparation procedure, which uses a series of progressively finer abrasives to create a scratch-free surface, must be meticulously carried out at each stage. A poor sample will come from carelessness at any point. The goal is to gently move from one stage to the next as the abrasives get progressively finer. In general, successive steps are 120,600,800,1200 and 2500 grit, grinding speed and force are kept constant from one stage to the next. The specimen's surface is first flattened using a rotating disc machine. These machines usually have coolant attachments to ensure cool cutting and aid in cleaning the disc of abrasive particles. During the rough grinding stage, caution should be taken to avoid the specimen becoming overheated. Before moving on to the next stage of the grinding process, the sample must be properly cleaned with ethanol or isopropanol. The process was done for eight times which equal to eight sections of specimens with each steps reducing the specimen by 0.5mm in height. This was done to analyse the microstructure of aluminium at different sections. Figure 5 shows the machine used for grinding and polishing process.

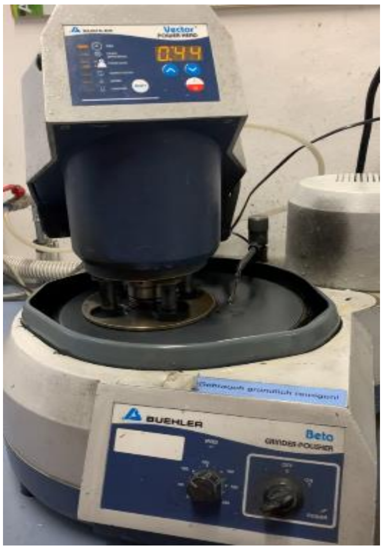

Figure 5. Grinding and polishing machine

The deep scratches created by the rough grinding abrasives are removed by polishing the sample. Any remaining defects should be reflective of flaws in the sample itself rather than a result of the metallographic preparation process as the surface turns shiny and reflective. The process is done using four different polishing discs starting with 9µm, 3µm, 1µm and OPS. The diamond suspension will act as lubricant during the process. For each of the polishing process, the diamond suspension must be adding every interval of 30 seconds until the process finish. Meanwhile for the OPS, the time taken to polish is 10 minutes where the first five minutes is polished using the suspension and the remaining five minutes is polished using only water.

In the context of fundamental research, the domains of material science, materials engineering, materials diagnostics, hardness testing is a crucial tool for analysis, differentiating between materials, developing, and improving materials and technologies. It establishes the characteristics that are significant for determining the suitability of a material for a technically core element, for differentiating various materials, and for defining damage cases (damage analysis). A material's hardness is a measure of how resistant it is to being mechanically penetrated by a harder body (indenter). In this experiment, Vickers hardness tests were done on the aluminium alloy specimens where a diamond is used as an indenter referring to Figure 6. The diamond indenter is in the shape of a square-based pyramid is pressed into the specimen's surface. The size of the resulting indentation is then measured under a microscope, and the Vickers hardness number (HV) is calculated based on the area of the indentation and the applied force. Based on Table 1, Specimen A has a smaller HV value compared to Specimen B. This shows that the smaller the indentation, the harder the material is.

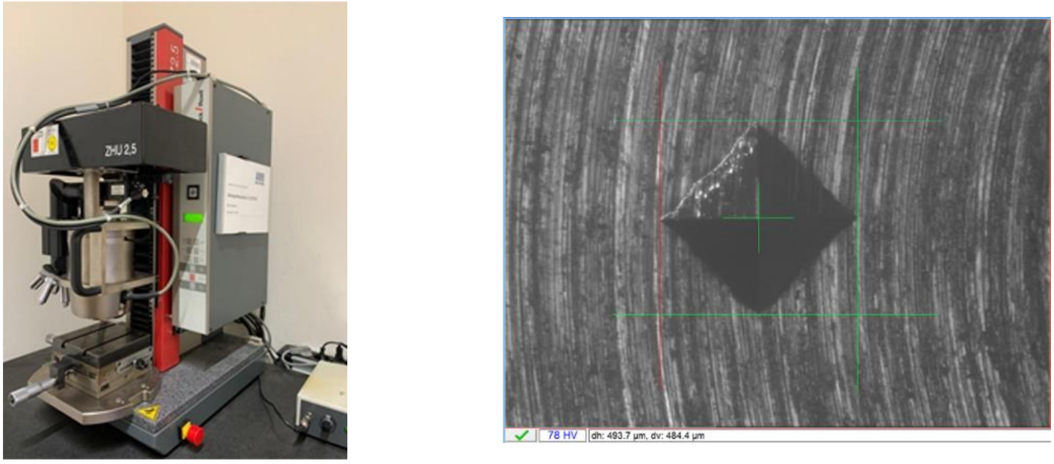

Figure 6. Hardness test – (a) Vicker hardness machine; (b) Diamond indentation

2.2 Analysis using open software ImageJ

ImageJ is a widely used open-source image processing software for analysing the microstructure images. It has a wide range of features for image analysis and processing, including image manipulation, filtering, segmentation, and measurement. By using ImageJ, it allows to measure and analyse various aspects of microstructure, such as pore size, shape, and distribution in aluminium alloy. Image taken by the microscope is then being imported into ImageJ. Here, the image of aluminium microstructure is converted into grayscale and it is important to calibrate the images before any measurements are made to ensure accurate results. Based on Figure 7, the threshold of the image is done which helps in dividing the image into two classes of pixels called “foreground” and “background”. Segmenting the images is the process of separating the objects of interest from the background. By doing this, the pores that exist on the aluminium samples surface can be easily calculated by applying image calculator tools in ImageJ to obtain the size area of the pores. Operation AND is done for the calculation of pore size area.

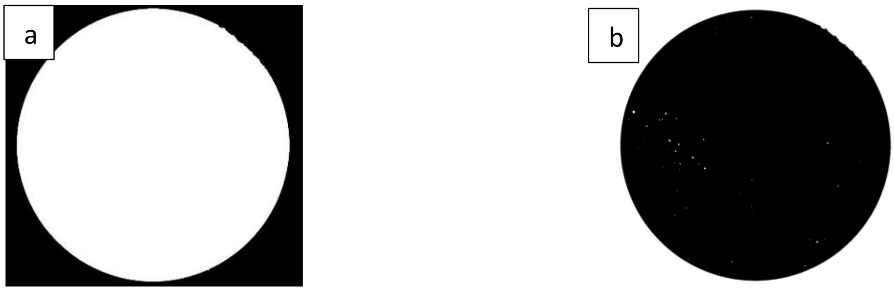

Figure 7. Threshold image - a) Foreground; b) Background

3.0 APPLICATION OF MURAKAMI METHOD

Statistical scatters of microstructures, defects and inclusion are the major factors of statistical scatters of fatigue strength and fatigue life. For the prediction of fatigue strength, the area of the maximum imperfection must be known. Material imperfections typically have irregular shapes that cannot be accurately represented by a circle or an ellipse. A technique developed by Yukita Murakami has been applied to predict the fatigue strength of metallic materials, including aluminium alloys, based on the crack closure concept. However, the method can also be extended to predict the fatigue behaviour of porous materials. Based on Figure 8, cutting the specimens into sections, the statics of extreme value of defects can be obtained. In particular, the maximum square root area of pores (MSRAP) has been identified as an important parameter affecting the fatigue strength of porous materials. The MSRAP is defined as the maximum square root area of all the pores in a unit volume of material. The crucial defect size decreases with increasing strength, so it is dependent on the hardness or ultimate tensile strength.

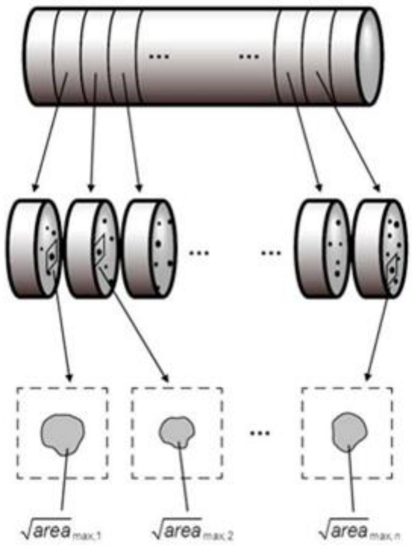

Figure 8. Data acquisition by each section [9]

The threshold condition at the fatigue limit is not for the initiation of a fracture but rather for the non-propagation of a crack originating from defects or inclusions, the effects of non-metallic inclusions must be examined from the perspective of small defects or small cracks. The equations for predicting the fatigue limit (σ_w) and the threshold stress intensity factor (ΔK_{th}) range for defects and small cracks were expanded to include inclusions found in high-strength steels to account for this problem. It is shown that the Vickers hardness, HV, of the matrix and the square root of the projected area of inclusions are the key factors in predicting the fatigue limit of metals having inclusions.

Using the Murakami method, the effective stress intensity factor range (ΔK_{eff}) can be calculated based on the cyclic stress-strain curve of the material. The method also takes into account the level of crack closure ($\Delta\sigma_c$) that occurs during each cycle of loading, which can be calculated based on the cyclic stress-strain curve and the effective stress intensity factor range. For porous materials, the MSRAP can be used to modify the effective stress intensity factor range with crack closure ($\Delta K_{eff'}$) calculated using the Murakami method [3]. The modified $\Delta K_{eff'}$ can then be used to predict the fatigue crack growth rate and fatigue life of the material using established fatigue crack growth models.

The square root of the defect projection area, $\sqrt{area}$, which is projected onto the plane perpendicular to the direction of maximum stress, is the most effective size parameter for defects because it has a strong correlation with the maximum stress intensity factor K_{max} at the crack font. Following are some examples of how an $\sqrt{area}$ expression for a surface fracture and subsurface crack might look. The stress intensity factor can be calculated using Equation (1) and Equation (2) [4] shown below.

$$K_{max} = 0.65\sigma \sqrt{\sqrt[\pi]{area}} \text{ for a surface crack} \quad (1)$$

$$K_{max} = 0.5\sigma \sqrt{\sqrt[\pi]{area}} \text{ for a subsurface crack} \quad (2)$$

From the perspective of fatigue, defects like inclusions or pores are similar to cracks. The relationship between fracture size and HV and the threshold stress intensity factors for small cracks is expressed as ΔK_{th} = C (HV + 120) ($\sqrt{area_{max}}^{1/3}$), where C = 3.3 x 10^{-3} for surface crack and for subsurface crack is modified by considering the relationship between Equation (1) and Equation (2). The Murakami method has been successfully applied to predict the fatigue behaviour of porous materials with different levels of porosity and MSRAP values. The method has also been used to optimize the microstructure of porous materials to improve their fatigue strength by controlling the MSRAP. The method for prediction strength of material by considering the maximum occurring pore size (area) and the Vickers hardness (as main responsible for the fracture mechanism) as basis of such calculations. The fatigue strength of specimen A and specimen B, σ_{FS}, can be calculated from Equation (3), where 1.43 is coefficient of surface crack while 1.56 in Equation (4) is the coefficient for subsurface defect [10].

$$\sigma_{FS} = \frac{1.43(HV+120)}{\sqrt{area_{max}}^{1/6}} \text{ (MPa) for surface crack} \quad (3)$$

$$\sigma_{FS} = \frac{1.56(HV+120)}{\sqrt{area_{max}}^{1/6}} \text{ (MPa) for subsurface crack} \quad (4)$$

4.0 RESULTS AND DISCUSSION

A microstructure image based on Figure 8 from a microscope after being polished shows the internal structure of the aluminium alloy at a high magnification. The grinding and polishing process of the surface of Specimen A and Specimen B to remove any surface irregularities or deformities, revealing the underlying microstructure. The resulting image based on Figure 9 shows the defects or form of inhomogeneities such as pores and inclusion appeared in the specimens. When fatigue is taken into consideration, failure happens at the biggest flaw or inhomogeneity found in the most stressed volume. Defects located at or close to the surface are more detrimental than internal ones. In real life, describing the fatigue strength of elements requires more information than just the defect size and applied stress. Therefore, fatigue failures in additive manufacturing materials start at surface defects. In this analysis, pores will be the interest in Murakami approach as it can act as stress concentrators, which can affect the overall strength and fracture behaviour of the material.

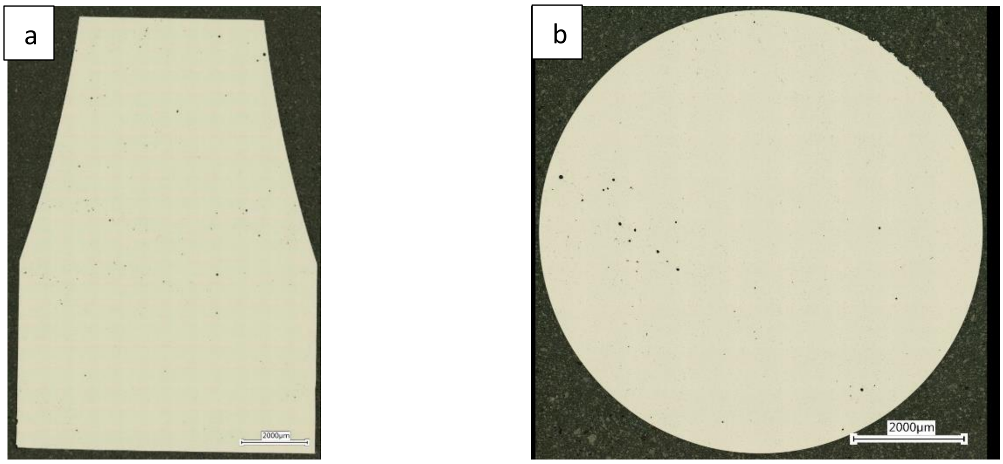

Figure 9. Microstructure of WAAM aluminium alloy - (a) Specimen A; (b) Specimen B

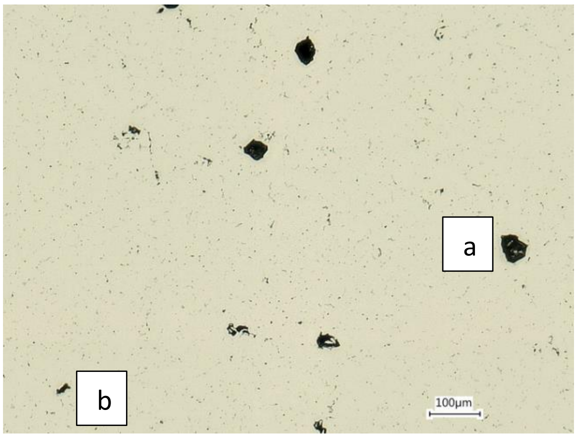

Figure 10. Defects in the WAAM aluminium alloy – a) pore; b) inclusion

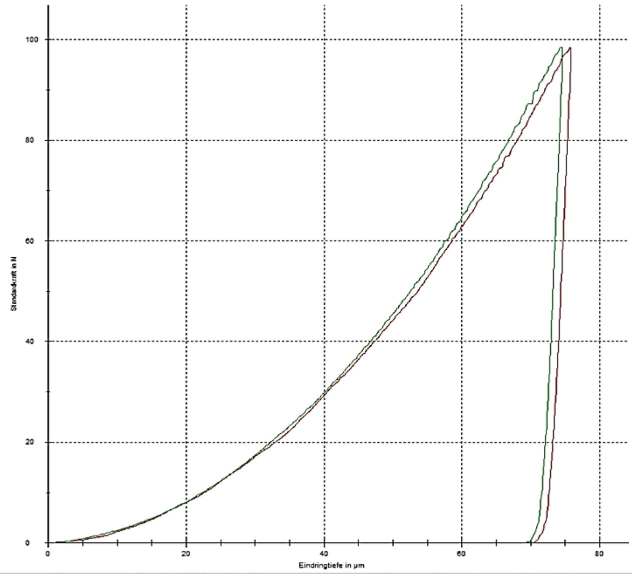

Legende	Nr	Index	d_h µm	d_v µm	d µm	HV 10	HIT_i N/mm²	EIT_i N/mm²	h_i µm	m	K N/mm²	$hmax_i$ µm	Ap_i mm²	F_i N	m(hi) kN/mm	m(hr) kN/mm	$HV(H_{IT})$
	1		513,61	501,45	507,5294	72,0				0,00	31406,03					31,41	-
	2		519,82	518,46	519,1407	68,8				0,00	33184,38					33,18	-

Figure 11. Hardness test on HS-Al-A

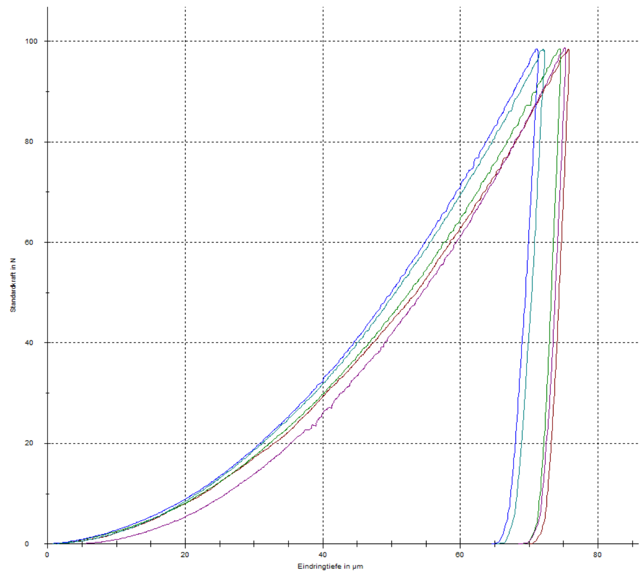

Legende	Nr	Index	d_h µm	d_v µm	d µm	HV 10	HIT_i N/mm²	EIT_i N/mm²	h_i µm	m	K N/mm²	$hmax_i$ µm	Ap_i mm²	F_i N	m(hi) kN/mm	m(hr) kN/mm	$HV(H_{IT})$
	1		513,61	501,45	507,5294	72,0				0,00	31406,03					31,41	-
	2		519,82	518,46	519,1407	68,8				0,00	33184,38					33,18	-
	3		483,20	492,24	487,7236	77,9				0,00	25707,73					25,71	-
	4		484,51	496,18	490,3438	77,1				0,00	25969,72					25,97	-
	5		491,05	484,38	487,7140	77,9				0,00	30812,38					30,81	-

Figure 12. Hardness test on HS-Al-B

Based on Fig.11 and Fig.12, the value of HV were obtained after hardness test were done on both of the specimens. The image processing using ImageJ on the specimens gives the result data of pore size area of each section of the material that has been grind and polished. The result data obtained by using the image calculator tools in ImageJ which perform arithmetic and logical operations between two threshold images, based on Figure 6. From the data, the fatigue strength analysis of the WAAM aluminium alloy using the Murakami method obtained by applying the Eq.1 with the value of hardness test HV in Table 1. By comparison HS-Al-A has a bigger pore size area than HS-Al-B. Referring to Figure 13, it shows that bigger area size will result in lower fatigue.

Table 1. Hardness test

	Specimen HS-Al-A	Specimen HS-Al-B
HV(kgf/mm^2)	70.4	74.7

Table 2. 8 sections of HS-Al-A

	1	2	3	4	5	6	7	8
MAX AREA (μm^2)	6210	7424	4153	2697	4014	4035	3294	2833
$\sqrt{area_{max}}$ (μm)	79	86	64	52	63	64	57	53
σ_{FS} (MPa)	131	130	136	141	136	136	139	140

Table 3. 8 sections of HS-Al-B

	1	2	3	4	5	6	7	8
MAX AREA (μm^2)	1931	835	1624	3804	1702	671	1249	3236
$\sqrt{area_{max}}$ (μm)	44	29	40	62	41	26	35	57
σ_{FS} (MPa)	150	161	153	142	152	162	156	144

Table 4. Average $\sqrt{area_{max}}$, σ_{FS} & stress intensity factor, K_{max} of specimens HS-Al-A and HS-Al-B

Specimen	HS-Al-A	HS-AL-B
σ_{FS} (MPa)	136.13	152.5
$\sqrt{area_{max}}$ (μm)	64.75	41.75
K_{max} (MPa·m$^{1/2}$)	333.75	325.13
ΔK_{th} (MPa·m$^{1/2}$)	2.52	2.26

Pores or voids are common features in metallic materials that can affect their mechanical properties, including fatigue strength. The size of pores can have a significant impact on the fatigue strength of the material. In general, large pores are likely to act as stress concentrators and initiate cracks, which can lead to failure. Additionally, smaller pores can be filled with the surrounding material during plastic deformation, reducing their size and minimizing their impact on the material's fatigue behaviour.

As a result, the fatigue strength of a material can decreases significantly with an increase in pore size. Large pores can also reduce the effective cross-sectional area of the material, leading to a decrease in the material's overall strength. However, the impact of pore size on fatigue strength also depends on the material's microstructure, loading conditions, and the location of the pores within the material. For example, pores located at the surface of a material may have a greater impact on the material's fatigue strength compared to those located deeper within the material. The orientation and shape of the pores can also affect their impact on the material's fatigue behaviour.

In addition to pore size, other factors such as the number and distribution of pores, the material's grain size and texture, and the presence of other defects or impurities can also affect the material's fatigue strength. Overall, the size of pores is an important factor affecting the fatigue strength of metallic materials. Minimizing the size and number of pores through appropriate material processing techniques can lead to improved fatigue strength and better performance of the material in service.

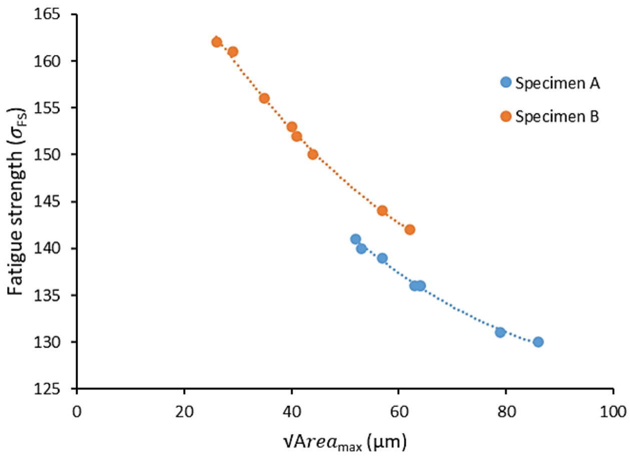

Figure 13. Graph of Fatigue strength vs $\sqrt{area_{max}}$ of WAAM aluminium alloy

5.0 CONCLUSION

This research focuses on the Murakami Method which is used to evaluate the fatigue strength of wire arc additive manufacturing (WAAM) aluminum. The highlight of the study is to find the relationship between the pore size and fatigue strength by using the $\sqrt{area_{max}}$ parameter for predicting the fatigue resistance of metallic materials. Larger pores or voids can lead to more severe stress concentrations and a higher likelihood of crack initiation, resulting in lower fatigue strength. If the projected area of inclusions onto the plane perpendicular to the maximum principal stress is the same as the area of a small crack, then the fatigue problem of inclusions is deemed equivalent to that of small cracks. In other words, the fatigue behaviour of inclusions within a material can be considered equivalent to that of small cracks. It is important to consider that the value of ΔK_{th} for inclusion (or an equivalent crack) depends on its size, specifically its $\sqrt{area}$. According to the results of this research, the following conclusion can be made:

1. Reliable estimation of fatigue strength requires accurately estimating the maximum occurring defect.
2. The pore size area can be assessed by using open-source software ImageJ by considering pixel and actual distance of the microstructure image of the WAAM aluminium as well as threshold value of the image.
3. Hardness values obtained by using Vicker's hardness test and maximum area of the defects are used as the Murakami basis in evaluating the fatigue strength.
4. Pores in a material's microstructure can act as stress concentrators, leading to lower fatigue strength.
5. By comparison, specimen B has a higher fatigue strength of 153 MPa compared to specimen A with 137MPa due the smaller pore size area in specimen B.
6. The method is valuable for analysing fatigue strength of metallic materials with different microstructures and porosity.

Overall, the Murakami Method provides a useful tool for predicting the fatigue life of engineering components, particularly in cases where experimental data is limited or unavailable. However, like any analytical method, its accuracy is dependent on the assumptions and simplifications made in the analysis, and its results should always be verified withexperimental data whenever possible.

ACKNOWLEDGEMENT

The authors would like to acknowledge the Chair of General Mechanical Engineering in Montanuniversität Leoben, ERASMUS+ KA107 and Smart Manufacturing Research Institute, Universiti Teknologi MARA for the continuous support and guidance through the research.

REFERENCES

[1] Y. Murakami, "Inclusion Rating by Statistics of Extreme Values and Its Application to Fatigue Strength Prediction and Quality Control of Materials.", *Journal of Research of the National Institute of Standards and Technology*, vol. 99, no. 4, July – August 1994.

[2] M. Jimenez-Martinez, "Manufacturing effects on fatigue strength," *Engineering Failure Analysis*, vol. 108, Jan. 2020, doi: 10.1016/j.engfailanal.2019.104339.

[3] J. C. Pang, S. X. Li, Z. G. Wang, and Z. F. Zhang, "General relation between tensile strength and fatigue strength of metallic materials," *Materials Science and Engineering: A*, vol. 564, pp. 331–341, Mar. 2013, doi: 10.1016/j.msea.2012.11.103.

[4] N. Sanaei and A. Fatemi, "Defects in additive manufactured metals and their effect on fatigue performance: A state-of-the-art review," *Progress in Materials Science*, vol. 117. Elsevier Ltd, Apr. 01, 2021. doi: 10.1016/j.pmatsci.2020.100724.

[5] L. Bercelli, S. Moyne, M. Dhondt, C. Doudard, S. Calloch, and J. Beaudet, "A probabilistic approach for high cycle fatigue of Wire and Arc Additive Manufactured parts taking into account process-induced pores," *Additive Manufacturing*, vol. 42, Jun. 2021, doi: 10.1016/j.addma.2021.101989.

[6] J. Lee, S. Y. Park, and B. H. Choi, "Evaluation of fatigue characteristics of aluminum alloys and mechanical components using extreme value statistics and C-specimens," *Metals (Basel)*, vol. 11, no. 12, Dec. 2021, doi: 10.3390/met11121915.

[7] T. Hauser *et al.*, "Porosity in wire arc additive manufacturing of aluminium alloys," *Additive Manufacturing*, vol. 41, May 2021, doi: 10.1016/j.addma.2021.101993.

[8] S. Beretta and Y. Murakami, "Statistical analysis of defects for fatigue strength prediction and quality control of materials," *Fatigue & Fracture of Engineering Materials & Structures* vol. 21, no. 9, pp. 1049–1065, 1998, doi: 10.1046/j.1460-2695.1998.00104.x.

[9] C. Xie *et al.*, "Defect-correlated fatigue resistance of additively manufactured Al-Mg4.5Mn alloy with in situ micro-rolling," *Journal of Materials Processing Technology*, vol. 291, May 2021, doi: 10.1016/j.jmatprotec.2020.117039.

[10] Y. Murakami, H. Masuo, Y. Tanaka, and M. Nakatani, "Defect Analysis for Additively Manufactured Materials in Fatigue from the Viewpoint of Quality Control and Statistics of Extremes," in *Procedia Structural Integrity*, Elsevier B.V., 2019, pp. 113–122. doi: 10.1016/j.prostr.2019.12.014.

[11] R. K. Rhein, Q. Shi, S. Arjun Tekalur, J. Wayne Jones, and J. W. Carroll, "Effect of direct metal laser sintering build parameters on defects and ultrasonic fatigue performance of additively manufactured AlSi10Mg," *Fatigue & Fracture of Engineering Materials & Structures*, vol. 44, no. 2, pp. 295–305, Feb. 2021, doi: 10.1111/ffe.13355.

[12] Y. Murakami, "Material defects as the basis of fatigue design," in *International Journal of Fatigue*, Aug. 2012, pp. 2–10. doi: 10.1016/j.ijfatigue.2011.12.001.

[13] P. Sharma, S. Sharma, and D. Khanduja, "A study on microstructure of aluminium matrix composites," *Journal of Asian Ceramic Societies*, vol. 3, no. 3, pp. 240–244, Sep. 2015, doi: 10.1016/j.jascer.2015.04.001.

[14] Y. Murakami and M. Endo, "Effects of defects, inclusions and inhomogeneities on fatigue strength," *International Journal of Fatigue*, Volume 16, Issue 3, Pages 163-182, April 1994.

[15] Y.Murakami and S.Beretta, "Small Defects and Inhomogeneities in Fatigue Strength: Experiments, Models and Statistical Implications". *Extremes 2*, 123–147,1999, https://doi.org/10.1023/A:1009976418553

[16] Y. Murakami, S. Kodama, and S. Konuma, "Quantitative evaluation of effects of non-metallic inclusions on fatigue strength of high strength steels. I: Basic fatigue mechanism and evaluation of correlation between the fatigue fracture stress and the size and location of non-metallic inclusions," International Journal of Fatigue, Volume 11, Issue 5, pp. 291-298, September 1998.

[17] A. Casagrande, G. P. Cammarota, and L. Micele, "Relationship between fatigue limit and Vickers hardness in steels," *Materials Science and Engineering A*, vol. 528, no. 9, pp. 3468–3473, Apr. 2011, doi: 10.1016/j.msea.2011.01.040.